

Structure and transport properties of $\text{La}_{1.85}\text{Sr}_{0.15}\text{Cu}_{1-x}\text{V}_x\text{O}_4 + \delta$

This article has been downloaded from IOPscience. Please scroll down to see the full text article.

2003 J. Phys.: Condens. Matter 15 5723

(<http://iopscience.iop.org/0953-8984/15/33/306>)

View [the table of contents for this issue](#), or go to the [journal homepage](#) for more

Download details:

IP Address: 171.66.16.125

The article was downloaded on 19/05/2010 at 15:04

Please note that [terms and conditions apply](#).

Structure and transport properties of $\text{La}_{1.85}\text{Sr}_{0.15}\text{Cu}_{1-x}\text{V}_x\text{O}_{4+\delta}$

L H Liu¹, G C Che and Z X Zhao

National Laboratory for Superconductivity, Institute of Physics, Chinese Academy of Science, PO Box 603, Beijing 100080, People's Republic of China

E-mail: liulihua@ssc.iphy.ac.cn

Received 29 May 2003

Published 8 August 2003

Online at stacks.iop.org/JPhysCM/15/5723

Abstract

The structure and transport properties of the V-doped $\text{La}_{2-x}\text{Sr}_x\text{CuO}_{4+\delta}$ system have been studied in this paper. The maximum doping concentration of V for Cu is 0.15 and a tetragonal-to-orthorhombic phase transition occurs at $x = 0.10$. Resistivity and magnetization measurements show that the V doping will depress the superconductivity in this system. The Kondo-like effect gives a good description of the temperature dependence of resistivity for all samples. The superconducting transition temperature T_c systematically shifts to lower temperature with increasing V concentration and disappears at a critical concentration $x_c = 0.15$. This x_c is much higher than that of the $\text{La}_{1.85}\text{Sr}_{0.15}\text{Cu}_{1-x}\text{M}_x\text{O}_{4+\delta}$ ($M = \text{Fe}, \text{Co}, \text{Ni}, \text{Zn}, \text{Mg}, \text{Al}$ and Ga) systems, in which T_c disappears when $x = 0.018\text{--}0.04$. A possible explanation for this phenomenon is presented. In addition, there exists a small concave section in the $T_c\text{--}x$ phase diagram around $x = 0.02$, very similar to the 1/8 behaviour in the $\text{La}_{2-x}\text{Sr}_x\text{CuO}_4$ system.

1. Introduction

Since the discovery of high- T_c superconductors, understanding their structure and transport properties has rapidly advanced due to the vigorous effort of both experimentalists and theoreticians [1–4]. With the simplest layered structure, $\text{La}_{1.85}\text{Sr}_{0.15}\text{CuO}_{4+\delta}$ is the focus of intense studies [5–9]. One way to probe the superconducting mechanism is to substitute Cu^{2+} ions by transition metals or other elements. Substitution experiments on Cu^{2+} ions by divalent and trivalent ions, such as Ni^{2+} , Zn^{2+} , Mg^{2+} , Fe^{3+} , Co^{3+} , Ga^{3+} and Al^{3+} , have been carried out by a number of groups [10–14]. A common result in all of these studies is that T_c is depressed in the same manner, independent of whether the dopant is magnetic or nonmagnetic. However, it remains unclear what mechanism is responsible for the T_c suppression. In the

¹ Author to whom any correspondence should be addressed.

1990s, Wallace *et al* [15–17] studied V-doped $\text{La}_{1.85}\text{Sr}_{0.15}\text{CuO}_{4+\delta}$ with V content ranging from 0 to 0.05. Further addition of V results in the formation of impurity phases and a tetragonal-to-orthorhombic transition. T_c decreases from 34 to 24 K as x increases from 0 to 0.04. To understand the degradation of superconductivity systematically, we extended the study to a higher doping level ($x \leq 0.15$). In this paper, the effect of V-doping on the structure of $\text{La}_{1.85}\text{Sr}_{0.15}\text{Cu}_{1-x}\text{V}_x\text{O}_{4+\delta}$ and the correlation of T_c with its normal-state transport properties were investigated.

2. Experiment

A series of $\text{La}_{1.85}\text{Sr}_{0.15}\text{Cu}_{1-x}\text{V}_x\text{O}_{4+\delta}$ ($x = 0.0\text{--}0.15$) samples were prepared by solid-state reaction from appropriate amounts of high-purity La_2O_3 , SrCO_3 , V_2O_5 and CuO . The La_2O_3 powder was calcined at 850°C before weighing. The starting materials were thoroughly mixed and calcined first at 900°C for 24 h in air to get the precursors. Then the precursors were reground and pressed into pellets. The pellets were heated at 960°C for 72 h and cooled down to room temperature at a rate of 30°C h^{-1} . All samples were prepared under identical conditions.

It is well known that V_2O_5 is a powder with a melting point of 658°C , whereas V_2O_4 has a melting point of 1640°C , and copper oxide (CuO) has a melting point of 1336°C . Above 700°C V_2O_5 dissociates into V_2O_4 and O_2 according to the following equations [18]:



Under the preparation conditions employed in this paper, V is likely to stay as V^{4+} in the materials.

The structure of the samples was analysed by powder x-ray diffraction using an MXP-AHF18 diffractometer. The data used for Rietveld refinement were collected by step scanning with a step width of 0.02° and counting times of 5 s. The lattice parameters were calculated by a least-squares method using the PowderX program [19]. Resistivity as a function of temperature between 10 and 300 K for all the prepared samples was measured using a standard four-probe method. All the magnetic measurements were done by using a Quantum Design superconducting quantum interference device (SQUID) magnetometer.

3. Results and discussion

3.1. Structure

X-ray diffraction indicates that all of the samples are single phase with good quality in the V-doping level of $0 \leq x \leq 0.15$. Figure 1 shows the XRD patterns for all specimens, in which no impurity phase can be observed. This indicates that the V dopant definitely substitutes in the Cu site. The maximum doping concentration (0.15) is much larger than that reported by Wallace *et al* [15–17].

For the samples with $x = 0.0, 0.020, 0.025, 0.05, 0.10$ and 0.15 , the x-ray diffraction data were analysed by the Rietveld structure refinement technique, using the program Rietan2000. All possible position (x, y, z), thermal (B), and occupancy (N) parameters were varied in addition to cell parameters and half-width parameters. Due to the correlations between the roughness and thermal parameters, they were varied in separate cycles. The occupancy of the La(Sr) site was refined by constraining the cation proportions to the nominal, namely 1.85:0.15. V ions were assumed to be in the V^{4+} state. The occupancy of Cu/V was refined by assuming

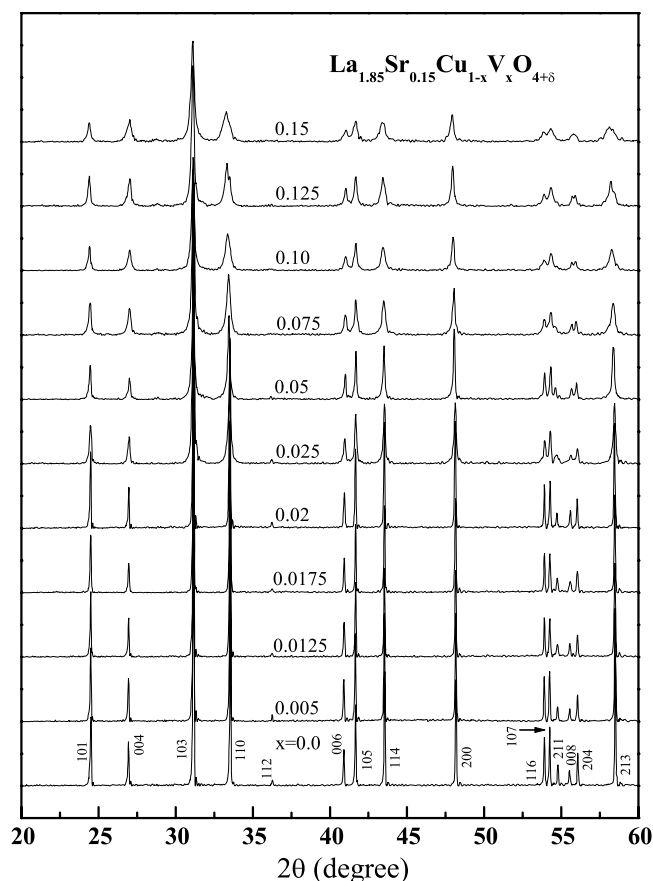


Figure 1. The x-ray diffraction patterns in the $\text{La}_{1.85}\text{Sr}_{0.15}\text{Cu}_{1-x}\text{V}_x\text{O}_{4+\delta}$ system for all specimens. No observable impurity peak is found.

full occupancy at the Cu site. The pseudo-Voigt-type diffraction profile was adopted during the refinement.

The observed and profile-fitted diffraction patterns, as well as the difference patterns for the compositions $x = 0.0, 0.02, 0.025, 0.05, 0.10$ and 0.15 , are shown in figure 2. A look at the difference patterns and the values of the R factors show that the fits are satisfactory. These results confirm that the V^{4+} indeed replaces Cu^{2+} . The structural parameters are shown in figure 3 as a function of x .

The crystal structure remains tetragonal with increasing V concentration from 0.00 to 0.10. The parameter a increases with the increase of x while c decreases, resulting in a progressive decrease in c/a . The observed lattice parameter variations are similar to those reported previously in Ni^{2+} -, Zn^{2+} -, Mg^{2+} -, Ga^{3+} -, Fe^{3+} - and Co^{3+} -doped $\text{La}_{1.85}\text{Sr}_{0.15}\text{CuO}_{4+\delta}$ systems.

The increase in the length of the a axis with increasing V content x suggests a decrease in the number of holes in the CuO_2 plane, resulting from the replacement of bivalent Cu^{2+} by polyvalent V^{4+} . This is probably linked with the decrease of T_c . Because the radii of V^{4+} (0.072 nm) is much smaller than that of Cu^{2+} (0.087 nm) in an octahedral environment, the parameter c therefore decreases as x increases. It is generally accepted that the c/a ratio is

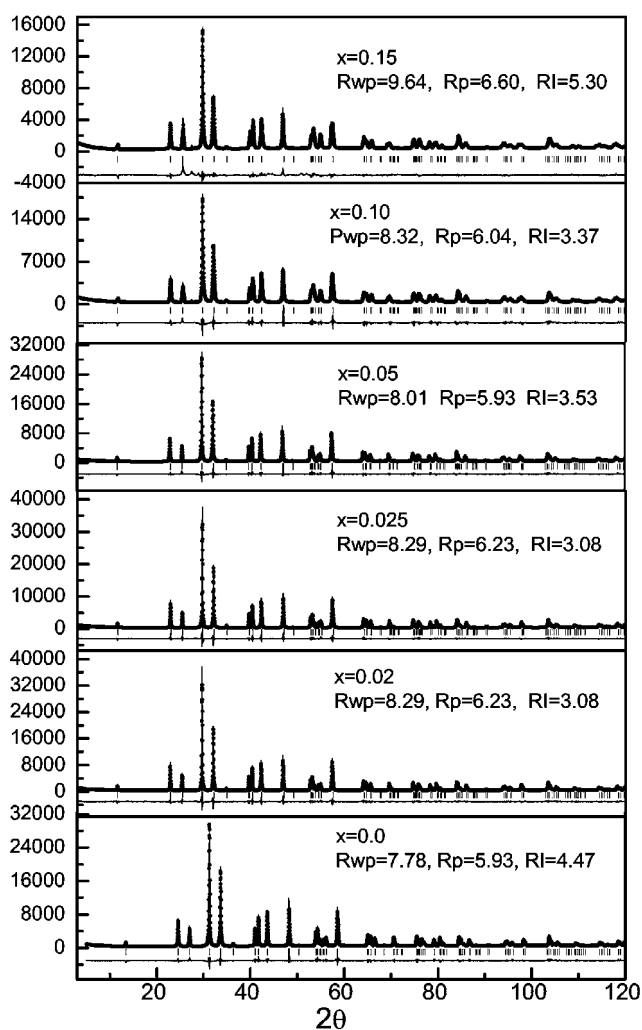


Figure 2. Rietveld refinement plots for $x = 0.0, 0.020, 0.025, 0.05, 0.10$ and 0.15 . The dots are the observed x-ray diffraction data and the full curve is the profile-fitted diffraction patterns. The difference patterns (observed results minus calculated ones) are plotted at the bottom. The tick marks below the pattern represent the position of all possible Bragg reflections.

used to characterize the Jahn–Teller distortion of the oxygen octahedron around Cu^{2+} . For the pure $\text{La}_{2-x}\text{Sr}_x\text{CuO}_{4+\delta}$ phase, the Cu–O bonds along the c axis are longer than those within the basal (a, b) planes. As the V^{4+} ion substitutes for the Cu^{2+} ion in the lattice, the CuO_6 octahedron is progressively squeezed along the c axis, which leads to a release of Jahn–Teller distortion, as in the $\text{La}_{1.85}\text{Sr}_{0.15}\text{CuO}_{4+\delta}$ systems doped by other metallic elements.

A tetragonal-to-orthorhombic phase transition occurs at a V content of 0.10, resulting from the mismatch between the CuO_2 and $(\text{La}, \text{Sr})_2\text{O}_2$ layers. This kind of phase transition also appears in the Zn-doped $\text{La}_{1.85}\text{Sr}_{0.15}\text{CuO}_{4+\delta}$ system [20]. The critical V content (0.10), corresponding to structural transition, is also larger than that reported in the paper [15–17]. We thought that the different experimental results probably originate from the different vanadium oxide used as reactant. Wallace *et al* thought that V substitutes the Cu^{2+} in the form of V^{3+} ,

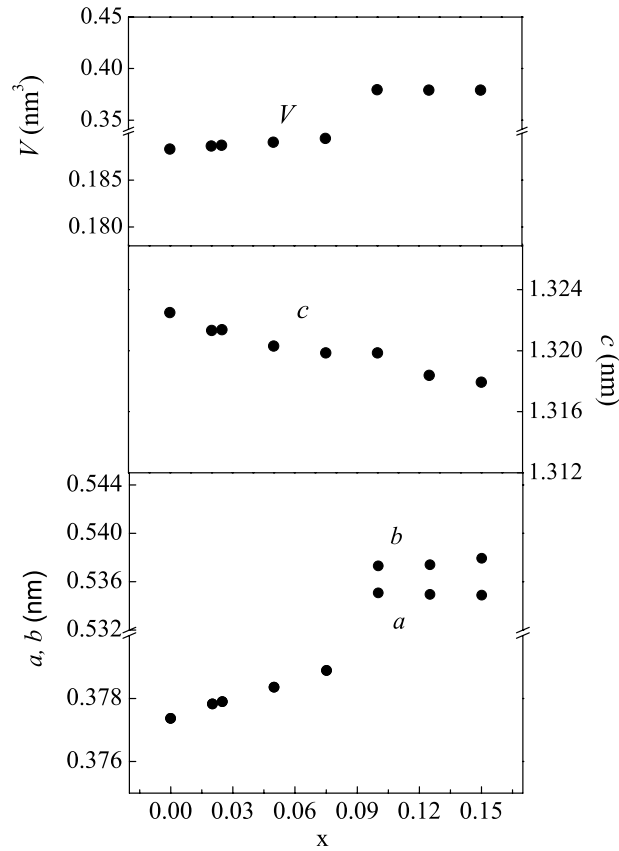


Figure 3. The structure parameters a , b and c and volume V as a function of x in $\text{La}_{1.85}\text{Sr}_{0.15}\text{Cu}_{1-x}\text{V}_x\text{O}_{4+\delta}$ determined by x-ray powder diffraction.

because V_2O_3 was used as the starting material of $\text{La}_{1.85}\text{Sr}_{0.15}\text{Cu}_{1-x}\text{V}_x\text{O}_{4+\delta}$. However, in the preparation of our samples, V_2O_5 instead of V_2O_3 was used as the starting material, so that V maybe exists in the V^{4+} state in our samples, as reported in [21] and discussed in section 2.

It has been established that the CuO_2 planar structure is highly susceptible to symmetry-lowering distortion. For example, the nonsuperconducting La_2CuO_4 is orthorhombic, resulting from the bending of Cu-O-Cu bonds in the CuO_2 planes. But hole doping by Sr substitution tends to destroy the distortion and makes the $\text{La}_{2-x}\text{Sr}_x\text{CuO}_4$ ($x > 0.06$) superconducting. In the optimally doped tetragonal $\text{La}_{1.85}\text{Sr}_{0.15}\text{CuO}_{4+\delta}$ phase the CuO_2 plane is flat and copper and oxygen atoms are distributed on a perfect square lattice. In our experiment, the addition of V reduces the symmetry and causes the tetragonal-to-orthorhombic phase transition. For the orthorhombic phase, the tilt of the Cu octahedron causes the movement of oxygen out of the CuO_2 plane, slightly distorting the Cu-O-Cu bond angle away from 180° . The structural distortion is known to substantially influence the density-of-state (DOS) near E_F [22]. Thermal expansion and neutron structural studies have also shown that the deformation of the CuO_2 planes by the octahedron tilt is detrimental to superconductivity [23, 24]. Therefore, the structural variation of the $\text{La}_{1.85}\text{Sr}_{0.15}\text{Cu}_{1-x}\text{V}_x\text{O}_{4+\delta}$ is probably another reason for the reduction of superconductivity.

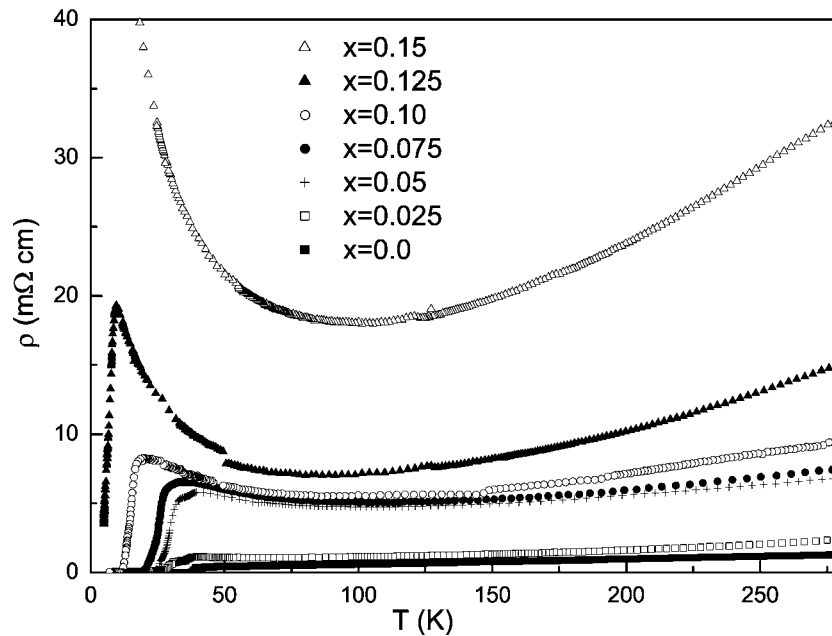


Figure 4. The resistivity versus temperature curves for all $\text{La}_{1.85}\text{Sr}_{0.15}\text{Cu}_{1-x}\text{V}_x\text{O}_{4+\delta}$ samples from 300 to 4.2 K.

3.2. Resistivity

The temperature dependence of the resistivity for some typical specimens is shown in figure 4. For the samples with $x \leq 0.025$, the high temperature resistivity has a metallic behaviour in a wide temperature range above T_c . The addition of more V has an effect on the normal-state resistivity both in the low and high temperature regions. There is a well-defined minimum followed by an upturn at the low temperature region. In the high temperature region, the resistivity increases nonlinearly. Such a behaviour has been observed in many transition-metal-doped $\text{La}_2\text{CuO}_{4+\delta}$ and $\text{YBa}_2\text{Cu}_3\text{O}_{4+\delta}$ compounds [10, 25, 26].

Figure 5 gives the room temperature resistivity $\rho(297)$ as a function of V content. The dependence of $\rho(297)$ on x indicates a dramatic increase, which is faster than that of Fe^{3+} -, Co^{3+} -, Ga^{3+} -, Ni^{2+} - and Zn^{2+} -doped $\text{La}_{1.85}\text{Sr}_{0.15}\text{CuO}_{4+\delta}$ [27]. Cieplak *et al* thought that the trivalent impurities reduced the number of hole carriers and so affected the resistivity more strongly than the divalent impurities, which have no influence on hole concentration. According to this idea, it is reasonable that the tetravalence V^{4+} will increase $\rho(297)$ more quickly than the divalent and trivalent impurities, as we observed in our experiment.

The characterization of the normal-state resistivity curves allows a comprehensive understanding of the electronic state of the doped holes. We first investigated the possibility of an activation behaviour and a variable-range hopping process. The resistivity associated with these mechanisms would show a temperature dependence as $\rho \sim \exp(T^{-\beta})$, with $\beta = 1, 1/4, 1/2$, corresponding to activation, uncorrelated and correlated variable-range hopping processes, respectively. However, the graphical analysis clearly revealed that the $\rho(T)$ anomaly is not described by these mechanisms since a straight line can be fitted only in a certain temperature range. Therefore, neither an activation process nor variable range hopping is responsible for the electronic transport properties.

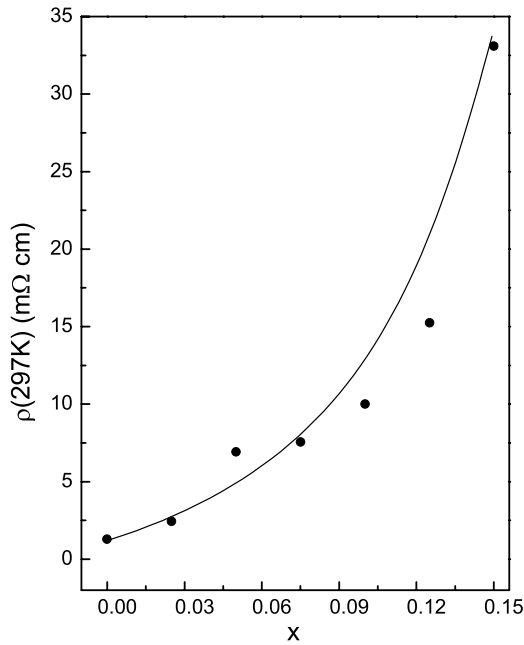


Figure 5. The room temperature resistivity $\rho(297\text{ K})$ as a function of the doping concentration x .

Another possible explanation for the observed resistivity behaviour is the Kondo-like effect. So we attempted to fit the resistivity data with the following relation:

$$\rho(T) = A + BT - C \ln(T). \quad (3)$$

Figure 6 presents the plots of $(\rho - A - BT)$ versus T on the logarithmic scale, for (a) samples with $x = 0.0, 0.025, 0.05, 0.075$ and 0.10 and (b) samples with $x = 0.10, 0.125$ and 0.15 . The curve for $x = 0.10$ is included in both cases for comparison.

As shown in figure 6, the above relation is well followed for all samples in the normal-state temperature range ($T_c < T < 300\text{ K}$). The fitted parameters, A , B and C are presented in figure 7 as a function of V concentration. All these parameters increase steadily with the increase of V concentration. According to equation (3), C/B is equal to the temperature T_{\min} , at which the resistivity has a minimum. In figure 8 we plot the values of C/B obtained by our fitting as well as the experimental values of T_{\min} . The agreement between these two sets of data indicates that the relation equation (3) accurately describes the electronic transport in our samples.

In the $\text{La}_{1.85}\text{Sr}_{0.15}\text{CuO}_{4+\delta}$ compound, the localized moment is very small and Kondo-like behaviour is not apparent. However, the localized paramagnetic moment on the Cu^{2+} site can be readily induced by the introduction of impurities according to the results of Xiao *et al* [14]. Each dopant of Fe^{3+} , Co^{3+} , Ni^{2+} , Zn^{2+} , Ga^{3+} and Al^{3+} either carries an intrinsic magnetic moment or induces a net moment on the CuO_2 plane. The addition of V^{4+} may also induce a moment as for the other metals and so made Kondo-like resistivity behaviour possible.

In order to determine the magnetic moment induced by the V^{4+} , we have measured the magnetic susceptibility with the variation of temperature for samples with compositions as labelled in figure 9. For clarity, the curves are shifted from each other by arbitrary values.

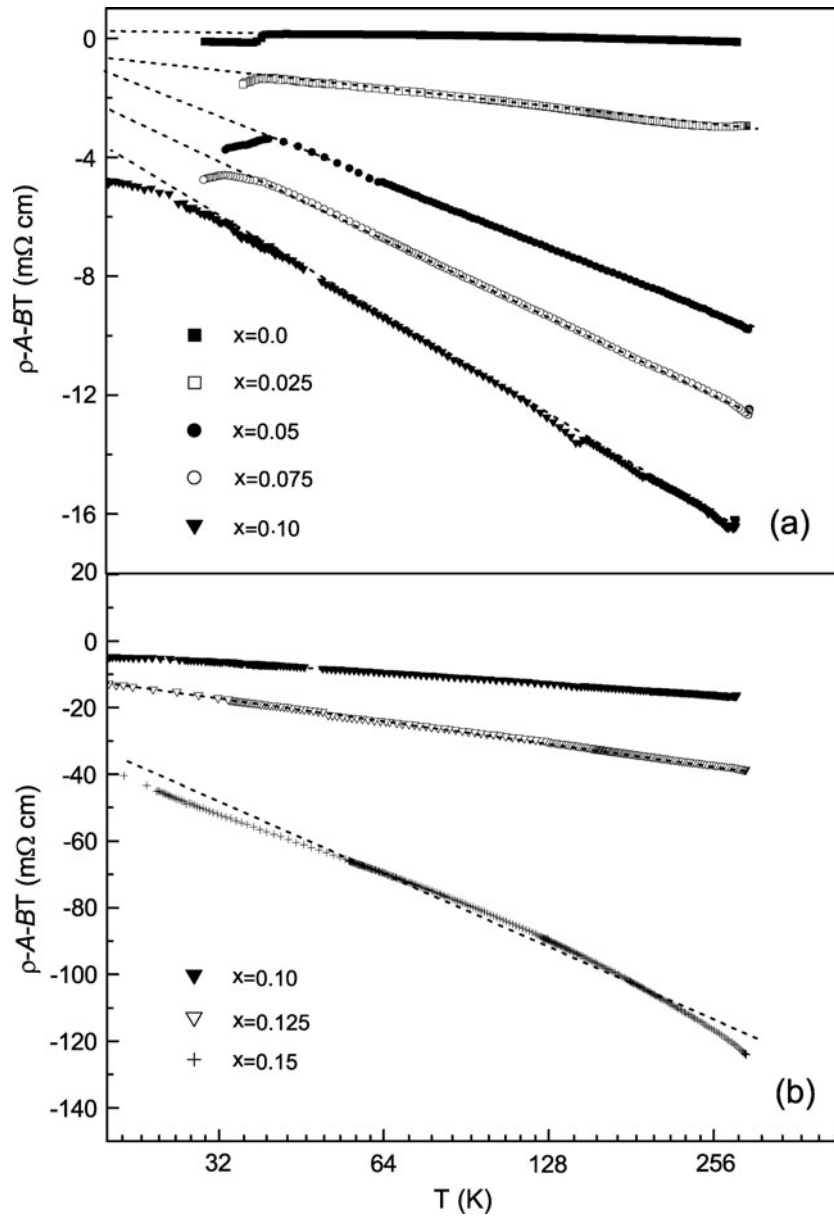


Figure 6. The dependence of the nonlinear part of the resistivity $\rho - A - BT = -C \ln(T)$ on $\ln(T)$ (see equation (3)) for samples (a) $x = 0.0, 0.025, 0.05, 0.075$ and 0.10 and (b) $x = 0.10, 0.125$ and 0.15 . The short broken lines represent the best fit of equation (3) to the experimental data.

The lines are fits to the data using the Curie–Weiss law

$$\chi = \chi_0 + \frac{N p_{\text{eff}}^2 \mu_B^2}{3k_B(T - \Theta)}, \quad (4)$$

where χ_0 is the temperature-independent part of the susceptibility, N is the number of magnetic ions, p_{eff} is the effective moment in units of Bohr magnetons μ_B and Θ is the Curie–Weiss

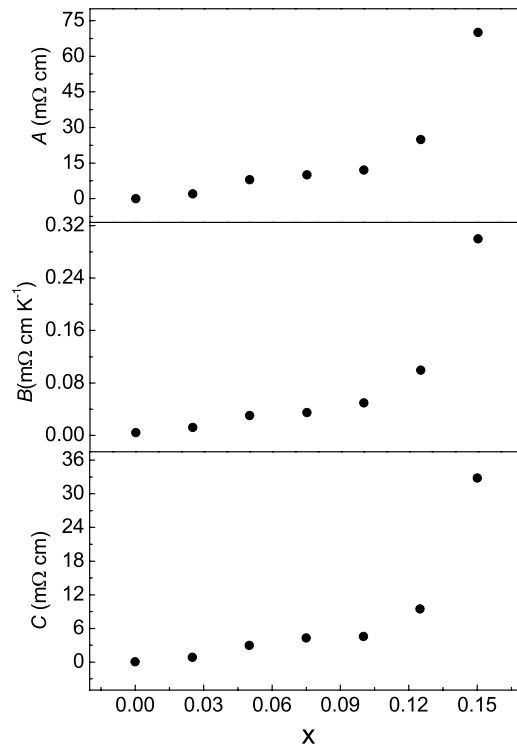


Figure 7. Variation of the fitted A , B and C parameters with the V content.

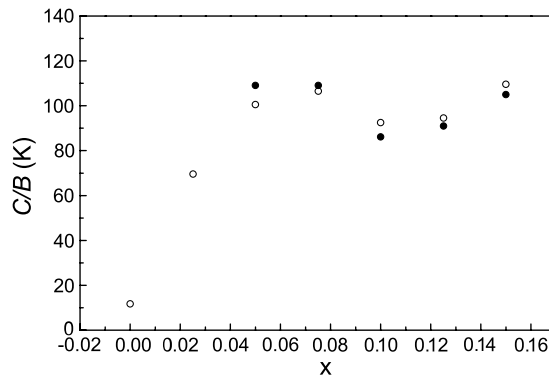


Figure 8. The ratio C/B obtained by the fitting (open circles) and experimental values of T_{\min} (filled circles) as a function of the V-doping level. The fitted values and the experimental values coincide with each other very well. For samples with $x = 0.0$ and 0.25 , there is no T_{\min} due to the linear behaviour of the resistivity above T_c .

temperature. The sudden drops in χ at low temperature for some samples are due to the superconducting transition. The p_{eff} obtained for a V^{4+} ion according to the above formula equals $0.7 \mu_B$ approximately.

It is generally accepted that the free holes, which are active charge carriers responsible for superconductivity, reside at the CuO_2 plane. Doping the Cu sublattice with V^{4+} will not only

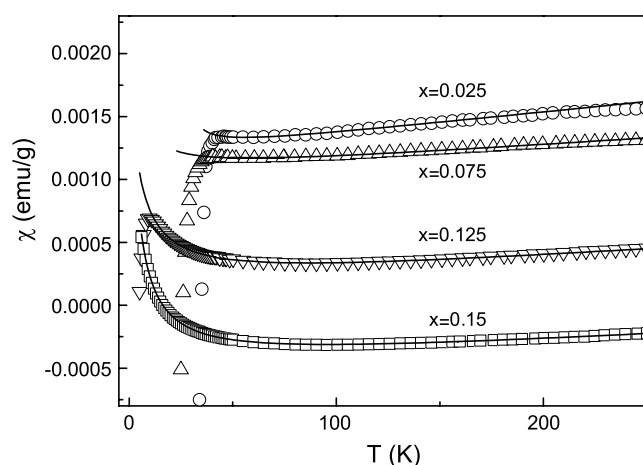


Figure 9. Magnetic susceptibility χ versus temperature for $\text{La}_{1.85}\text{Sr}_{0.15}\text{Cu}_{1-x}\text{V}_x\text{O}_{4+\delta}$ ($x = 0.025, 0.075, 0.125, 0.15$) samples. The curves are fits using the Curie–Weiss law.

destroy the structure, but also induce a localized moment ($\sim 0.7 \mu_B$) in the Cu^{2+} sites. As a result, the V-doped CuO_2 planes are, in many respects, a Kondo-like system. So it is reasonable that the Kondo-like resistivity behaviour occurs in the V-doped $\text{La}_{1.85}\text{Sr}_{0.15}\text{Cu}_{1-x}\text{V}_x\text{O}_{4+\delta}$ system.

3.3. Magnetization

The magnetization of the samples has been measured in the field-cooled mode (Meissner signal). The sample was first cooled down from room temperature to 5.5 K in a field of 10 Oe, and then the data were collected in the heating process up to 50 K. Figure 10 shows the magnetization curves as a function of temperature for some typical specimens.

With increasing x , the diamagnetic signal reduces gradually and disappears when $x = 0.15$, consistent with the resistivity result. The decrease of the diamagnetic signal with the increasing of x was also found in the other metal-doped $\text{La}_{1.85}\text{Sr}_{0.15}\text{CuO}_{4+\delta}$ systems. An explanation for this effect has been proposed by Junod *et al* [28].

3.4. T_c

Figures 11(a) and (b) show the variation of T_c (the temperature where the value of dM/dT or $d\rho/dT$ is maximum) as a function of x obtained from resistivity measurements and magnetization measurements, respectively. The two curves vary in a similar manner with V content. The x dependence of the superconducting transition temperature is nonlinear for our specimens, inconsistent with that in the other metal (Fe^{3+} , Co^{3+} , Ga^{3+} , Al^{3+} , Zn^{2+} , Mg^{2+} , Ni^{2+})-doped $\text{La}_{1.85}\text{Sr}_{0.15}\text{CuO}_{4+\delta}$ systems, in which T_c varies linearly with x . There exists a concave shape in the T_c - x phase diagram, very similar to the $1/8$ behaviour of the $\text{La}_{2-x}\text{Sr}_x\text{CuO}_4$ system [29–31] which possibly could be understood from the variation of the carrier concentration due to the V^{4+} doping.

In the $\text{La}_{2-x}\text{Sr}_x\text{CuO}_{4+\delta}$ system, the carrier concentration is correlated not only with the doping of the cation but also the anion. Taking no account of the oxygen, the addition of one V^{4+} ion will remove two free holes. Thus the hole concentration p when $x = 0.02$ is 0.11.

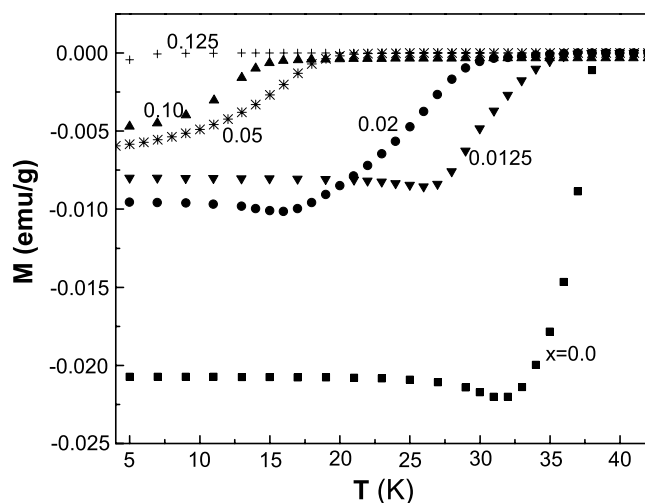


Figure 10. The temperature dependence of the magnetization for some typical specimens in $\text{La}_{1.85}\text{Sr}_{0.15}\text{Cu}_{1-x}\text{V}_x\text{O}_{4+\delta}$. The sample was first cooled down from room temperature to 5.5 K in a field of 10 Oe, and then the data were collected in the heating process up to 50 K.

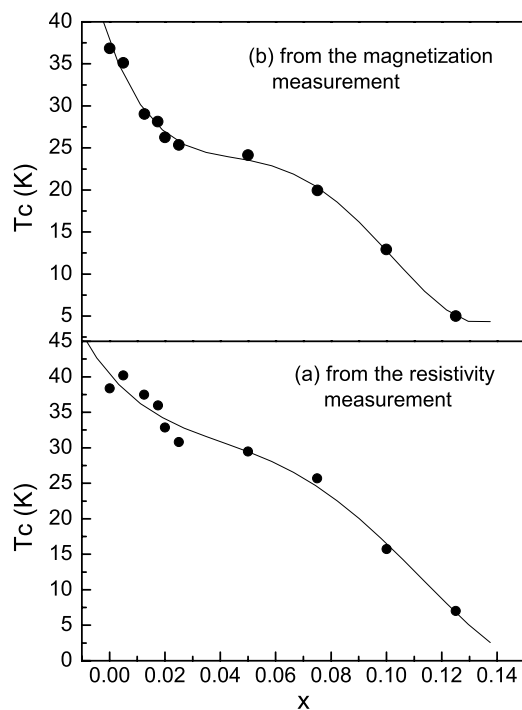


Figure 11. The variation of T_c as a function of x obtained from (a) resistivity measurements and (b) magnetization measurements.

However, due to the existence of excess oxygen δ , the actual hole concentration must be larger than 0.11. So it is probable that $p \sim 0.125(1/8)$ around $x \sim 0.02$, where the concave shape exists.

The critical doping level x_c at which T_c reduces to zero is 0.15, much larger than the x_c values (0.018–0.04) for the Fe^{3+} -, Co^{3+} -, Ga^{3+} -, Al^{3+} -, Zn^{2+} -, Mg^{2+} - and Ni^{2+} -doped $\text{La}_{1.85}\text{Sr}_{0.15}\text{CuO}_{4+\delta}$ systems. A result from [14] is that, for the divalent and trivalent cations, the degree of suppression of T_c is correlated with the size of the magnetic moment on the CuO_2 plane induced by the dopants, rather than the valence of the dopants. They found that x_c increases from 0.018 to 0.04 with the decrease of the induced magnetic moment p_{eff} from 5 to $0.6 \mu_B$. According to the above calculation, the p_{eff} obtained for a V^{4+} ion in our system equals $0.7 \mu_B$ approximately. Considering the large x_c (~ 0.15) in our V-doped samples, the conclusion made by Xiao *et al* [14] is not applicable in our system.

In the La_2CuO_4 -type compounds the $\text{Cu}(3d^9)$ has an empty $d_{x^2-y^2}$ orbit with spin 1/2. Nonmagnetic dopants, such as Zn^{2+} , Ga^{3+} , Al^{3+} and Mg^{2+} , have a full-shell structure ($3d^{10}$ or $2p^6$). Their main effect is to locally remove the spin-1/2 of $\text{Cu}^{2+}(3d^9)$. According to the magnetic measurement, the Co^{3+} ion in $\text{La}_{1.85}\text{Sr}_{0.15}\text{Cu}_{1-x}\text{Co}_x\text{O}_{4+\delta}$ is in the low-spin state with $S = 0$, while dopants such as Fe^{3+} and Ni^{2+} have high-spin states of $S = 5/2$ and 1, respectively.

Without exception, every dopant mentioned above will change the spin 1/2 of Cu^{2+} , and then destroy the antiferromagnetic correlation of the CuO_2 plane. This kind of magnetic disorder is extremely detrimental to high- T_c superconductivity. However, the V^{4+} ion only has one 3d electron and so spin $S = 1/2$. It seems possible that the substitution of Cu^{2+} by V^{4+} has a smaller effect on the antiferromagnetic ordering than the other metals. This is probably one reason for the slow decrease of T_c in the V-doped system.

4. Conclusions

The doping effect of V in the $\text{La}_{1.85}\text{Sr}_{0.15}\text{CuO}_{4+\delta}$ system has been studied in this paper. The maximum doping concentration of V for Cu is 0.15 and a tetragonal-to-orthorhombic phase transition occurs when $x = 0.10$. Resistivity and magnetization measurements show that the doping of V destroys the superconductivity. The logarithmic upturn in the resistivity indicates that neither an activation process nor variable range hopping is responsible for the low temperature electronic transport. The Kondo-like effect gives a very good description of the temperature dependence of the resistivity for all samples. T_c systematically shifts to lower temperature with increasing V concentration and disappears at a critical doping level $x_c = 0.15$. It is much higher than that of the $\text{La}_{1.85}\text{Sr}_{0.15}\text{Cu}_{1-x}\text{M}_x\text{O}_{4+\delta}$ ($M = \text{Fe}, \text{Co}, \text{Ni}, \text{Zn}, \text{Mg}, \text{Al}$ and Ga) systems, in which T_c 's disappear when $x = 0.018$ – 0.04 . A possible explanation for this phenomenon is presented. In addition, there exists a concave area in the T_c - x phase diagram around $x = 0.02$, very similar to the 1/8 behaviour in the $\text{La}_{2-x}\text{Sr}_x\text{CuO}_4$ system.

References

- [1] Torrance J B, Bezinge A, Nazzal A I, Huang T C, Parkin S S, Keane D T, LaPlaca S J, Horn P N and Held G A 1989 *Phys. Rev. B* **40** 8872
- [2] Axe J D, Moudden A H, Hohlwein D, Cox D E, Mohanty K M, Moodenbaugh A R and Xu Y 1989 *Phys. Rev. Lett.* **62** 2751
- [3] Oh-Ishi K and Syono Y 1991 *J. Solid State Chem.* **95** 136
- [4] Torardi C C, Subramanian M A, Gopalakrishnan J and Sleight A W 1989 *Physica C* **158** 465
- [5] Takagi H, Ido T, Ishibashi S, Uota M and Uchida S 1989 *Phys. Rev. B* **40** 2254
- [6] Torrance J B, Tokura Y, Nazzal A I, Bezinge A, Huang T C and Parkin S S P 1988 *Phys. Rev. Lett.* **61** 1127
- [7] Phillips J C and Rabe Karin M 1991 *Phys. Rev. B* **44** 2863

- [8] Takagi H, Cava R J, Marezio M, Batlogg B, Krajewski J J, Peck W F, Bordet P and Cox D E 1992 *Phys. Rev. Lett.* **68** 3777
- [9] Nagano T, Tomioka Y, Nakayama Y, Kishio K and Kitazawa K 1993 *Phys. Rev. B* **48** 9689
- [10] Tarascon J M, Greene L H, Barboux P, McKinnon W R and Hull G W 1987 *Phys. Rev. B* **36** 8393
- [11] Xiao G, Bakhshai A, Cieplak M Z, Tesanovic Z and Chien C L 1989 *Phys. Rev. B* **39** 315
- [12] Kang W, Schulz H J, Jerome D, Parkin S S P, Bassat J M and Odier P 1988 *Phys. Rev. B* **37** 5132
- [13] Xu G, Mao Z, Jin H, Yan H and Zhang Y 1998 *Phys. Lett. A* **249** 153
- [14] Xiao G, Cieplak M Z, Xiao J Q and Chien C L 1990 *Phys. Rev. B* **42** 8752
- [15] Wallace J B and King H W 1994 *J. Can. Ceram. Soc.* **63** 266
- [16] Wallace J W, Payzant E A, King H W, Stroink G and Dahn D C 1991 *J. Appl. Phys.* **69** 4587
- [17] King H W, Payant E A, Smith S W and Wallace J B 1995 *Supercond. Sci. Technol.* **8** 883
- [18] Clark R J H 1968 *The Chemistry of Titanium and Vanadium* (Amsterdam: Elsevier)
- [19] Dong C 1999 *J. Appl. Crystallogr.* **32** 838
- [20] Ganguly R, Rajagopal H, Sequeira A and Yakhmi J V 2000 *J. Supercond.* **13** 163
- [21] Salem A A, Sharaf El-deen L M and Elkholy M M 1999 *J. Mater. Sci. Lett.* **18** 71
- [22] Pickett W E, Cohen R E and Krakauer H 1991 *Phys. Rev. Lett.* **67** 228
- [23] Yamada N and Ido M 1992 *Physica C* **203** 240
- [24] Braden M, Hoffels O, Schnelle W, Buechner B, Heger G, Hennion B, Tanaka I and Kojima H 1993 *Phys. Rev. B* **47** 12288
- [25] Hasegawa T, Kishio K, Aoki M, Ooba N, Kitazawa K, Fueki K, Uchida S and Tanaka S 1987 *Japan. J. Appl. Phys.* **26** L337
- [26] Kang W, Schulta H J, Jerome D, Parkin S S P, Bassat J M and Odier Ph 1988 *Phys. Rev. B* **37** 5132
- [27] Cieplak M Z, Guha S, Kojima H, Lindendorf P, Xiao G, Xiao J Q and Chien C L 1992 *Phys. Rev. B* **46** 5536
- [28] Junod A, Ecjert D, Graf T, Triscone G and Muller J 1989 *Physica C* **162–164** 1401
- [29] Axe J D, Moudden A H, Hohlwein D, Cox D E, Mohanty K M, Moodenbagh A R and Xu Y 1989 *Phys. Rev. Lett.* **23** 2751
- [30] Katana S, Funahashi S, Mori N, Ueda Y and Fernandez-Baca J A 1993 *Phys. Rev. B* **48** 6569
- [31] Phillips J C and Rabe K M 1991 *Phys. Rev. B* **44** 2863